Comparative study on capped SiO_2 and TiO_2 to improve efficiency in plasmonic solar cell through modified synthesis approach

P. Sarkar[a,*], S. Panda[b], B. Maji[a], A. K. Mukhopadhyay[c]
[a]*Department of ECE, National Institute of Technology, Durgapur-713209, India*
[b]*Department of ECE, Dr. Sudhir Chandra Sur Institute of Technology & Sports Complex, Kolkata-700074, India*
[c]*Margadarshak (Mentor), AICTE, New Delhi -110070, India*

This study investigates the effectiveness of plasmonic improvement on photonic absorber properties of capped SiO2 and TiO2 nanoparticle in thin film a-Si photovoltaic cell. It also examines their J-V properties when exposed to sunlight. The modified Stober approach was used for irradiation tests, revealing lower reflectivity in different doses with SiO2 1st dose:0.485mg/ml, SiO2 2nd dose:0.693mg/ml, and TiO2 1st dose:0.525 mg/ml, TiO2 2nd dose:0.748 mg/ml solutions. Silica-based solar cells showed a 2.45% efficiency improvement, while titania-based solar cells improved efficiency by 0.657% compared with the uncoated sample.

(Received September 26, 2023; Accepted January 3, 2024)

Keywords: Plasmon, Silica, Titania, Solar cell

1. Introduction

The Industrial Revolution transformed energy production, transportation, and consumption, but it's causing environmental damage and depletion of natural sources like fossil fuels. Transitioning to clean energy sources like nuclear and renewables can reduce carbon emissions, but safe storage is challenging due to radioactive wastes long half-life. Green energy trends are increasing. Solar energy is a promising renewable source with minimal environmental impact and high efficiency. The solar photovoltaic industry reached a record delivery capacity of 295 GW in 2022, increasing the total global installed PV capacity to more than 1,198 TW [1]. Research and development focus on improving light conversion efficiency and reducing costs to meet global energy demand. The current worldwide photovoltaic solar cell market is 90% crystalline silicon-based, with 10% made up of thin films of polycrystalline semiconductors [2,3]. Thin film photovoltaic cell is growing as an alternate due to their low material consumption, flexibility, ease of integration, and suitability for large-scale production [4,5]. Thin film hydrogenated a-Si solar cell has low fabrication costs, simple processes, and compatibility with various substrates but lack efficiency.

Thin film Si solar cell reduce costs by reducing material and processing energy through photonic absorption methodologies, increasing optical path-length within thin layer [6]. Plasmonics is a growing field of nanotechnology that uses nanoparticles to improve solar cell absorption by scattering photons on nano-dimensions. It has been developing due to the availability of reliable synthesis and characterization processes [7,8,9]. Numerus Research teams have investigated several nanoparticle synthesis approaches, including chemical synthesis(CS) of coated film, e-beam lithography(EBL), and metal-island nano-structures(MIS) [10,11,12,13,28]. Metal nanoparticles have been found to act as resonators, absorbing and converting light into surface plasmons and excitation electrons in semiconductor materials, thereby increasing light absorption [7,8,12,13,14,15]. The scattering capacities of nanoparticles are influenced by their geometry, particle distribution, composition, and their surroundings medium's refractive index [9,16,17,18,38,39,40]. Surface plasmonic resonance (SPR) resonance can be tuned by optimizing attributes, with drude metals like titanium, aluminium, copper, gold, chromium, and silver

* Corresponding author: parthasarkar.info@gmail.com
https://doi.org/10.15251/JOR.2024.201.1

commonly used [19,20,21,22,23,35,36,37]. Metal nanoparticles are utilized in photonic absorption on photovoltaic cell front surfaces to minimize absorption loss. Scientists have created nanoparticle coatings that absorb and scatter specific wavelengths to reduce their absorption in dipolar resonance wavelengths, enabling precise light control in cell layers [24]. Minimizing scattering reduction can be achieved by enhancing size and shape to enhance radiative efficiency [25]. Dielectric nanoparticles are suitable due to their negligible scattering at optical wavelengths compared to metallic nanoparticles. Increased silica nanoparticle size increases optical absorption, leading to increased photocurrent production. Dielectric nanoparticles like silica, titania, and alumina are promising materials. The impact of silicon nanoparticles on photovoltaic silicon absorption and production has been investigated in electromagnetic scattering [28]. Photonic absorption can decrease cell efficiency in thin, sensitized layers, prompting research on improving device design and collection efficiency due to photonic absorption [26]. Dielectric nanoparticles exhibit lower ohmic loss and better phase matching compared to metal nanoparticles in subsequent layers structure, enhancing electron-hole pair collection from absorbed photonic spectrum.

2. Experimental methodology

Among various synthesis methodology of silica (SiO2) and titania (TiO2) nanoparticles, the Stober method is most popular and cost effective than Phytochemical method, and Co-precipitation method etc. Stober method is a variation of the hydrolysis sol-gel method that uses Tetra-Ethyl Ortho-Silicate (TEOS) as the precursor and ethanol and ammonia as the solvents and catalysts. The reaction produces spherical SiO2 nanoparticles with uniform size distribution [27, 28]. Stober method uses a hydrolysis sol-gel process to synthesize titania nanoparticles by reacting tetra isopropyl titanate (TIPT) precursors with different oxygen donor molecules such as alcohol solvent. The resulting nanoparticles have different crystalline phases and morphologies depending on the reaction conditions [29]. For both synthesis of silica and titania nanoparticles, the process steps are same in Stober method. The processing flow diagram is shown below.

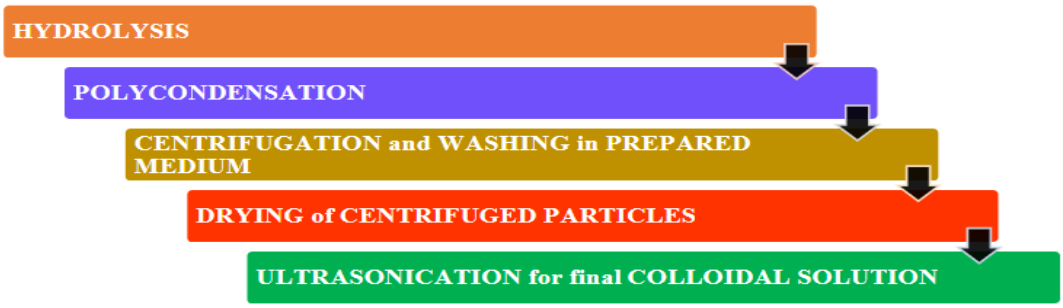

Fig. 1. Flow diagram of modified Stober sol-gel method.

2.1. Synthesis of Silica Nanoparticles using modified Stober Method

The Stober approach, a popular synthesis methodology, is adapted to create silica nanoparticles [28,30]. The Stober method was used to synthesize nano spherical SiO2 morphology by mixing 6 ml of 98% Tetraethyl Orthosilicate (TEOS) dropwise with 3 ml of 30% ammonium hydroxide in a solvent like ethanol or isopropanol, resulting in the desired size and morphology. The reaction can be allowed to proceed for several hours until the desired size is as small as 300nm and the morphology of the silica particles is achieved. After getting the desired morphology, the SiO2 solution goes through the following steps: initially centrifugation and washing in milky-white solution 2-3 times, then drying of centrifuged nanoparticles at 50^0C for 5 hours, finally, ultrasonication in the desired medium for a final colloidal solution [28]. The

synthesis of nano spherical SiO2 at the desired size and morphology has been taken in the subsequent steps below.

$$\text{Hydrolysis: } Si(OC_2H_5)_4 + 4H2O \xrightarrow[\text{maintain pH 11-12 ammonia}]{\text{mixed in ethanol}} Si(OH)_4 + C_2H_5OH$$

$$\text{Polycondensation: } Si(OH)_4 \xrightarrow[\text{maintain pH 11-12 ammonia}]{\text{added in aquas alcoholic medium}} SiO_2(sol) + 2H_2O$$

The deposited SiO2 nanoparticles are spin coated on a silicon surface with alcohol-based solution with a speed of 200 rpm to obtain a uniform coating of silica nanoparticles on the silicon surface [28]. This modified Stober procedure is widely used and can be applied to various materials, such as ethanol or isopropanol, to achieve the desired size and morphology of nano-spherical SiO2.

2.2. Synthesis of Titania Nanoparticles using modified Stober Method

The agglomeration of titania nanoparticles has been adopted with the Stober method. Hydrolysis steps involved adding 20 ml of solution tetra isopropyl titanate (TIPT) at a concentration of 98% to alcoholic solutions containing 10 ml of iso-propanol ($(CH_3)_2CHOH$) at 99% concentration and 12 ml deionized water values under constant agitated with a magnetic stirrer for 1 hour at 80^0C. Concentrate Nitric acid (HNO_3) has been added to maintain pH values 1-3 to maintain acidity. Under polycondensation, this solution was constantly stirred 6 hours to 8 hours at approx. 60^0C to get sol-gel of Titanium hydroxide ($Ti(OH)_4$) to result in the precipitation of Titanium dioxide (TiO_2). After centrifuging, TiO2 were washed several times in various concentration of isopropyl solutions and ultrasonically exposed in an alcoholic medium to form a colloidal solution for the particle. The synthesis of TiO_2 nanoparticles at the desired size and morphology has been taken in the subsequent steps below

$$\text{Hydrolysis: } Ti(OC3H7)4 + 4H2O \xrightarrow[\text{maintain pH 1-3 nitric acid}]{\text{suspension\_in\_water}} Ti(OH)_4 + 4C_3H_7OH$$

$$\text{Polycondensation: } Ti(OH)_4 \xrightarrow[\text{maintain pH 1-3 nitric acid}]{\text{suspension\_in\_water}} TiO_2(sol) + 2H_2O$$

Titania nanoparticles in isopropanol are spin-coated on a bare Si surface at 180 rpm to create TiO2 nanoparticles. Transparent conductive oxide (TCO) layers are required to ensure low resistive carrier transport to metal electrodes while acting as an anti-reflective coating. To avoid any contact between the TCO and the Al electrode, both Titania (TiO2) and silica (SiO2) -capped glass substrates were placed between two thin Al plates, and the clips and scotch tape were used to hold the electrodes in place. The TCO plate and the aluminium plate are attached between the metal probes.

3. Morphological characteristics and results

The plasmonic extinction affects absorption and scattering behaviours, with backscattering and front scattering additively influenced by particle size, direction, and environment, resulting in estimated optical scattering and extinction. [28,31,36,37,38,40,41,42]. The photonic scattering and extinctions can be defined as

$$\sigma_{sca} = \frac{2\pi}{k^2}\sum_{l=0}^{\infty}(2l+1)(|a_l|^2 + |b_l|^2) \quad (1)$$

and

$$\sigma_{ext} = \frac{2\pi}{k^2}\sum_{l=0}^{\infty}(2l+1)Re(a_l + b_l) \quad (2)$$

where k is wavevector defined as $k = 2\pi\sqrt{\varepsilon_m}/\lambda$, a_l and b_l are known as scattering or Mie Coefficients, defined by Ricatti-Bessel functions, where l is an index ranging from 1 to ∞ [16,18,19,31,32,33,34,36,37,41,42] and the average wavelength of solar irradiance(AM1.5) spectra, denoted by λ, is influenced by the optical extinction efficiency, Qext.. The average particle sizes can be estimated using solar irradiance absorption spectra, as shown in equation 2 [28]

$$R = \frac{\lambda}{\sqrt{2Q_{ext}}}\sqrt{\sum_{l=0}^{\infty}(2l+1)Re(a_l + b_l)} \quad (3)$$

Figure 2 and Figure 3 illustrate the FDTD simulation of a localized surface plasmonic effect in a solar cell containing SiO2 and TiO2 nanoparticles passivated transparent conductive oxide (TCO) layers on silicon under the presence of a normalized electric field with various wavelength λ= 400nm, 500nm, 600nm and 700nm respectively. Absorption enhancement has been found over a wide wavelength range due to plasmonic effect.

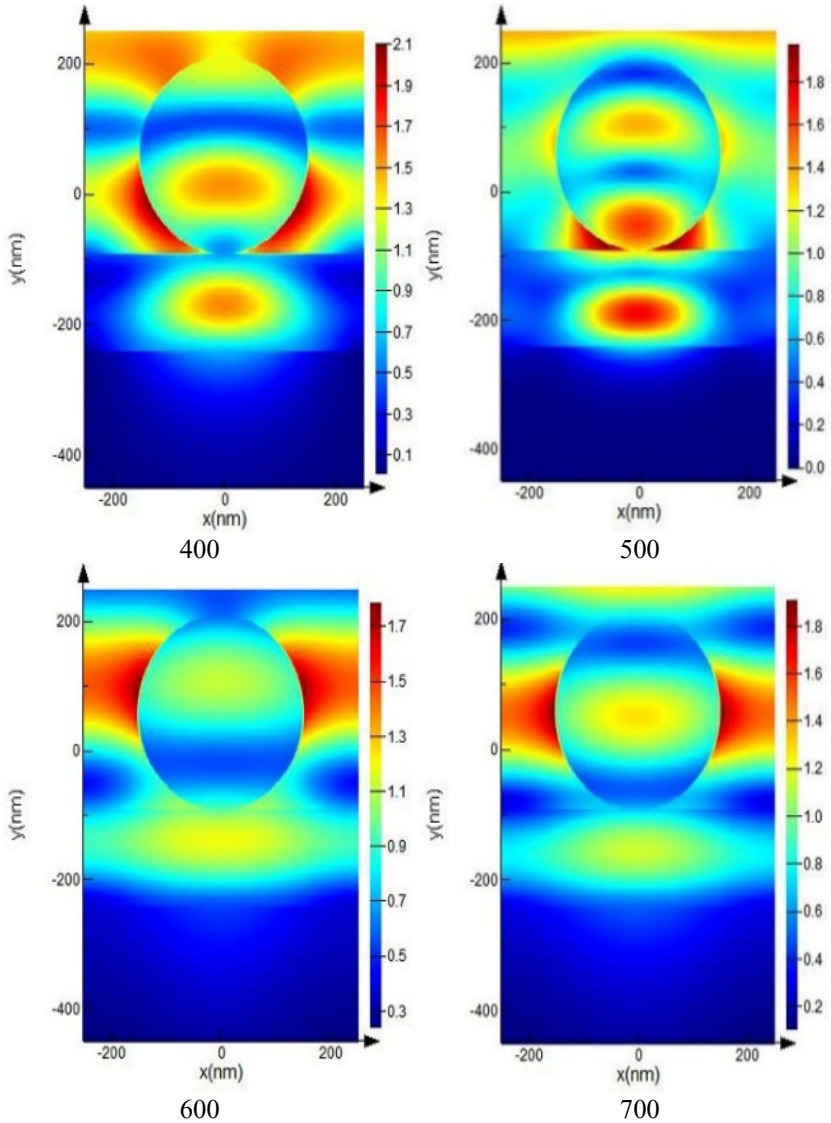

Fig. 2. FDTD simulation illustrate plasmonic effect due to SiO_2 nanosphere on thin-film silicon solar cell under solar irradiance.

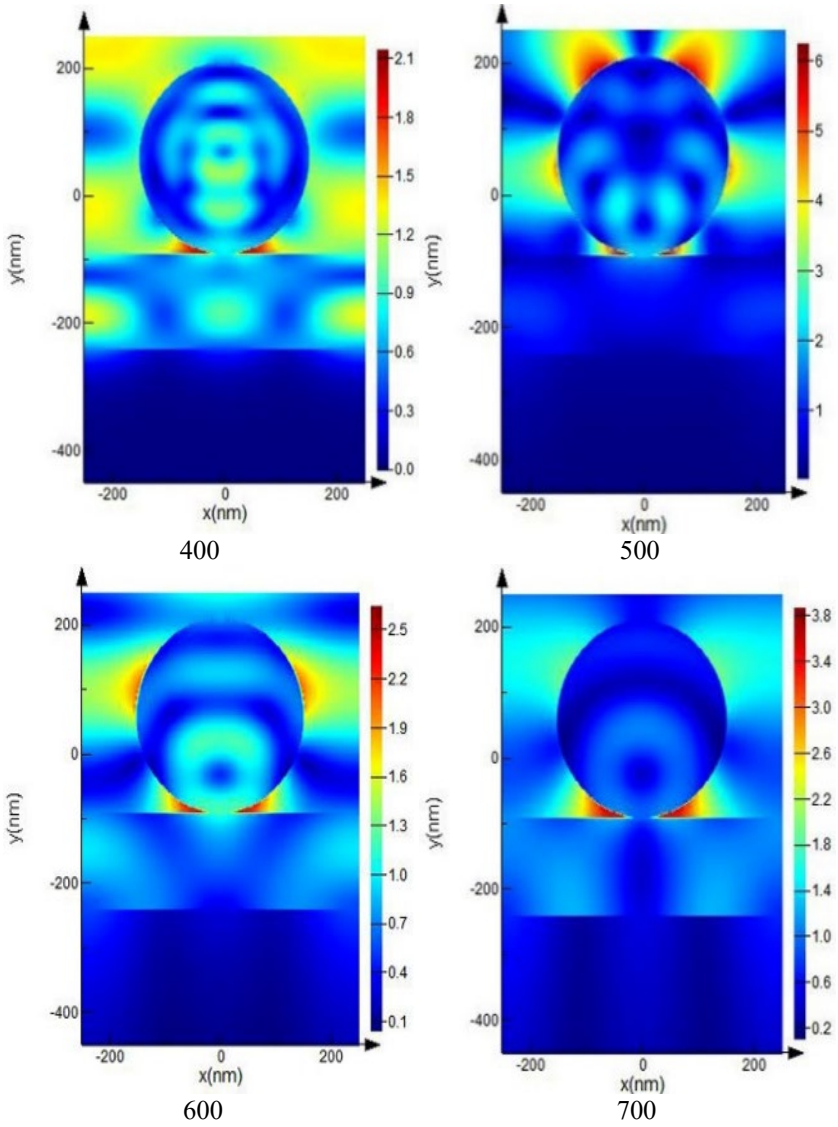

Fig. 3. FDTD simulation illustrate plasmonic effect due to TiO_2 nanosphere on thin-film silicon solar cell under solar irradiance.

The substrate's reflection characteristics were measured using a Bentham PVE300, and the desired illumination was achieved using a 300-watt Xenon lamp at AM1.5 with 100mWcm-2 irradiance [28]. Figure 4a illustrates the relationship between reflectance and irradiance wavelength for different SiO2 coating solutions with varying dosages that have a direct influence on covering area.

The results demonstrate that all silica doses significantly reduce light reflections compared to bare surfaces. The reflectance decreases with an increase in dosage at a specific particle size. The reflection characteristics of silica nanoparticles and infrared (IR) range, reflection reduces as results in an improvement in broadband absorption due to dipole oscillation. Silica nanoparticles, in ethanol dosages, are spin coated on bare Si surface at a speed, varies from 200rpm to 1500rpm, achieving uniform coverage. The reflection characteristic of titania nanoparticles with different colloidal dosages from 0.15ml solution, 0.45ml solution, 0.55ml solution and 0.75ml sample solution with wavelength ranging from 300mnm to 1100 nm is shown in figure 4b

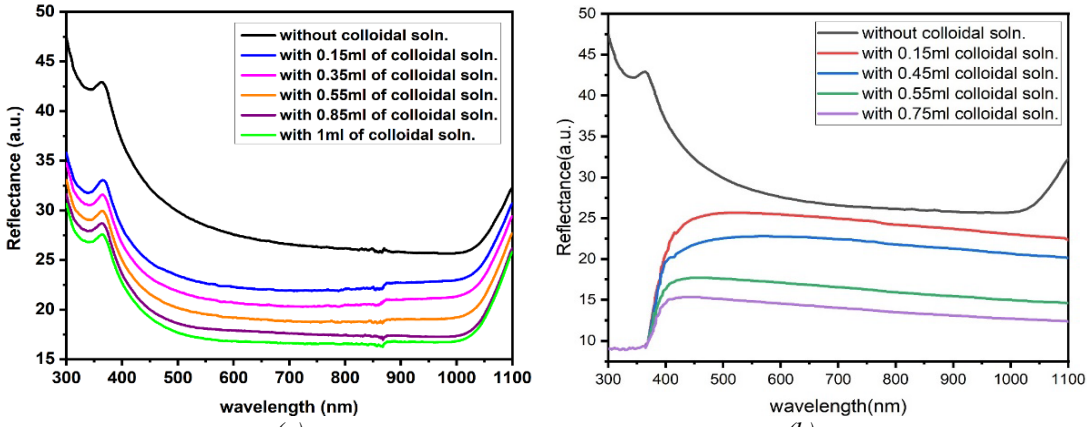

Fig. 4. (a) Reflectance vs. wavelength (varies from 300nm to 1100nm) with bare surface and coated different silica colloidal dosages: with 0.15ml solution, 0.35ml solution, 0.55ml solution, 0.85ml solution and 1ml solutions samples [28]. (b) Reflectance vs. wavelength (varies from 300nm to 1100nm) with bare surface and coated different titania colloidal dosages: with 0.15ml solution, 0.45ml solution, 0.55ml solution, 0.75ml solution samples.

The UV-VIS spectrophotometer (Perkin Elmer Lamda 35) was used to measure the absorption band of synthesized silica and titania nanoparticle specimens. Figure 5a shows UV-Visible absorption spectroscopy reveals silica nanoparticle coating doses with varying coverage density of 0.485mg/ml, 0.693mg/ml and 1.027mg/ml. Figure 5b represents the UV-Visible absorption spectra of irradiated titania samples show a noticeable enhancement in their absorption band, specifically in ultra-violet range with compared to the various dosages of colloidal solution of 0.525mg/ml, 0.748mg/ml, and 0.836mg/ml.

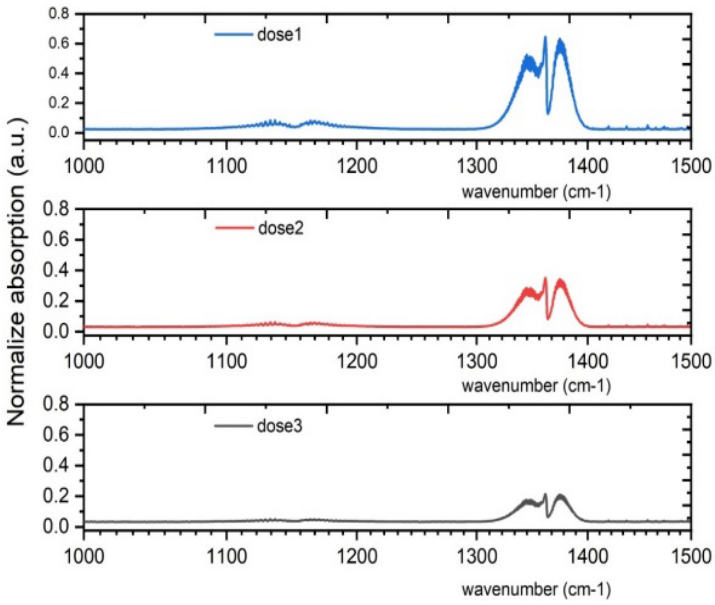

Fig. 5. (a) UV-Vis absorption spectra of SiO2 spin coated doses:
(i) dose 1: 0.693mg/ml, (ii) dose 2: 0.485mg/ml, (iii) dose3: 1.027mg/ml [28].

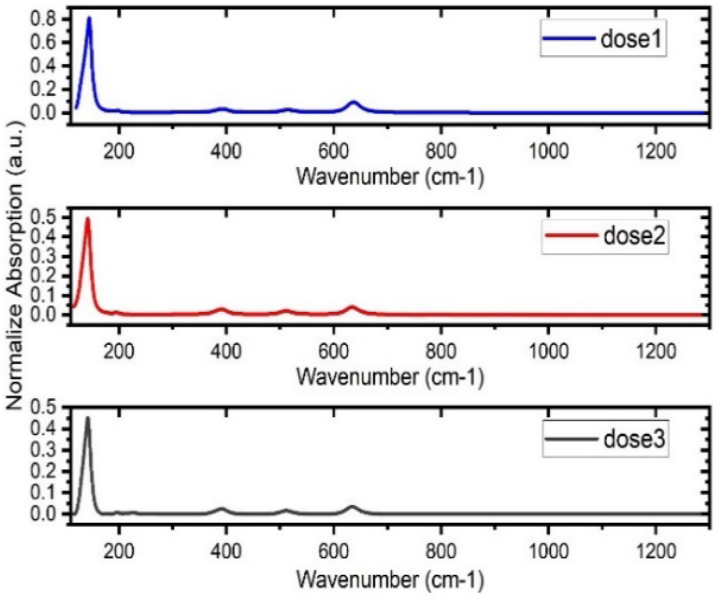

(b)

Fig. 5. (b) UV-Vis absorption spectra of TiO2 spin coated doses:
(i) dose 1: 0.525mg/ml, (ii) dose 2: 0.748mg/ml, (iii) dose3: 0.836mg/ml.

The morphological nanostructure of SiO2 and TiO2 nanoparticles was measured using an XRD spectrometer (Bruker AXS with a Cu Kα source and a λ= 0.15406). According to the Debye-Scherrer equation, Figure 6a depicts amorphous nanocrystals of silica nanoparticles that relate to two theta glancing angles at a broad angle of 24.8°.

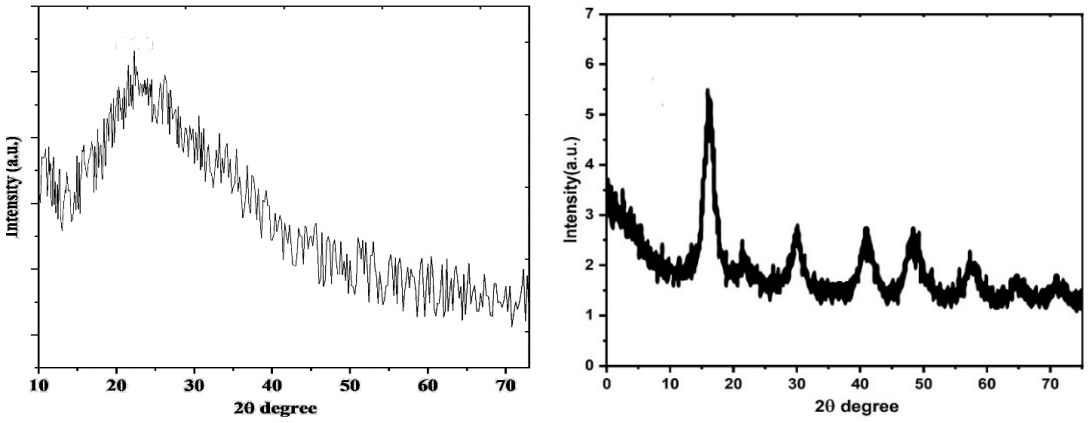

(a) *(b)*

Fig. 6. (a) XRD spectrum of SiO2 nanoparticales in coating solution at dose1: 0.693mg/ml.(b) XRD spectrum of TiO2 nanoparticales in coating solution at dose1: 0.525mg/ml.

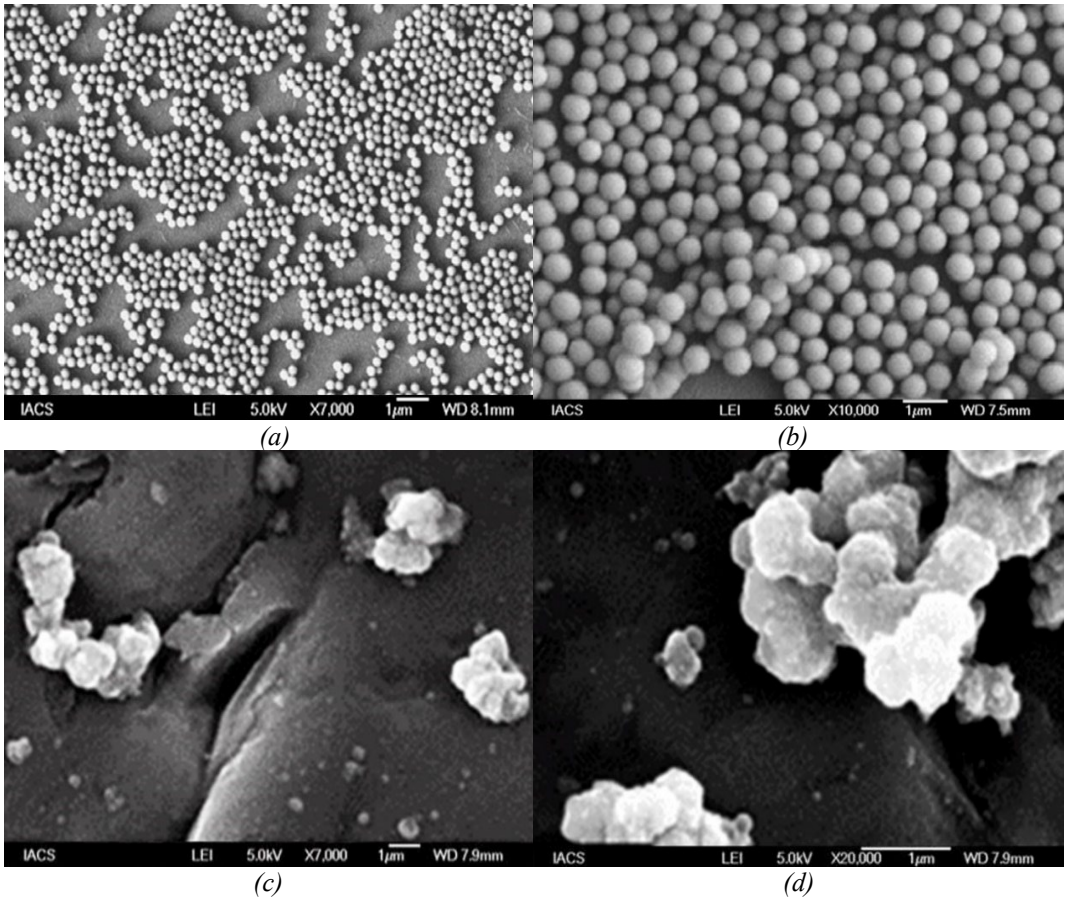

Fig. 7. Field Emission Scanning Electron Microscope (FESEM) image of SiO2 and TiO2 samples with (a) SiO2 1st dose: 0.693mg/ml solution, (b) SiO2 2nd dose: 0.485mg/ml solution [28], (c) TiO2 1st dose: 0.525 mg per ml solution, (d) TiO2 2nd dose: 0.748 mg per ml solution.

The significant decrease in reflectivity is achieved by forming a thin and smooth capped layer of SiO2 on the substrate by spinning it at 480 rpm to 500 rpm with a coating solution of 0.693 mg per ml. The experiment reveals that the size of SiO2 varies from 83nm to 106nm with amorphous crystallinity. Figure 6b shows XRD, an x-ray diffraction plot of TiO2 nanoparticles that contain several peaks primarily due to anatase and rutile crystalline phases at prepared amorphous titania. Anatase polymorphs has better photonic absorption feature than rutile crystalline phase. FESEM image of morphological size and shape of SiO2 and TiO2 nanoparticles with different colloidal dosages shown in figure 7.

The FESEM image shows that SiO2 nanoparticles are nanospherical in shape [28], whereas the FESEM image clearly shows that the surface morphological structure of TiO2 capped size is not spherical like SiO2. That directly impacts the efficiency of solar cells as backscattering is more dominant than front scattering.

4. Discussions

The AM1.5 illumination standard measures the J-V characteristic of photovoltaic cells, while photovoltaic cell efficiency (PCE) is calculated using electrical variables like open-circuit voltage, short-circuit current density, and fill factor as below.

$$\eta = \frac{FF.J_{SC}V_{OC}}{Pin} \tag{4}$$

Figure 8 illustrates the J-V characteristics of thin-film si-solar cells (TFSi-SC) with various spin-coating dosages of SiO2 and TiO2 nanoparticles.

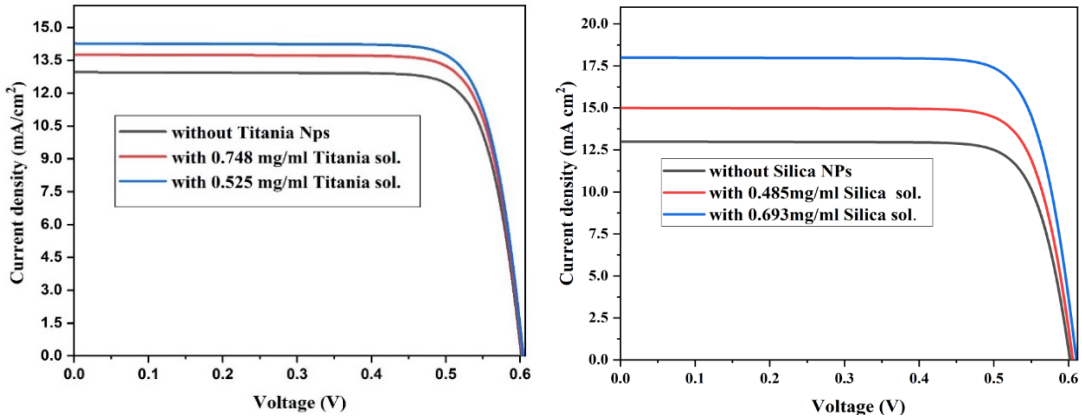

Fig. 8. J-V curve of photovoltaic cells with varying dosages on capped sensitizer SiO2 and TiO_2 nanoparticles.

Among the silica sample doses, the best improvement in reflection was achieved with a thin layer of agglomerated silica coated at 480 rpm for 0.693mg/ml dosage, resulting in greater efficiency and J-V characteristics under solar irradiation. Table 1 shows the comparison between photovoltaic electrical parameters such as Jsc, Voc, FF and PCE for various dielectric concentrations without and with silica and titania dosages, respectively.

Table 1. Calculation of J-V parameters of TFSi-SC at different SiO_2 and TiO_2 dosages.

Dielectric Coating	**Coating**	**J_{sc} ($mAcm^{-2}$)**	**V_{oc} (Volts)**	**FF**	**PCE (η%)**
Bear surface	No coating	12.95	0.601	0.8014	6.24
Silica 1st dose	0.693 mg/ml solution	17.89	0.611	0.7954	8.69
Silica 2nd dose	0.485 mg/ml solution	14.99	0.610	0.7991	7.30
Titania 1st dose	0.525 mg/ml solution	14.27	0.604	0.7999	6.897
Titania 2nd dose	0.748 mg/ml solution	13.76	0.603	0.8005	6.646

From the comparative studies from the table, SiO2 1st dose: 0.693mg/ml and SiO2 2nd dose: 0.485mg/ml, the improvement in short-circuit current (Jsc) is approximated at 3.78% and 1.56%, respectively, with compared to the bare sample. For titania coating, TiO2 1st dose: 0.525 mg/ml and SiO2 2nd dose: 0.748 mg/ml, the enhancement in short circuit current (Jsc) goes up to 1.01% and 0.62%, compared with the uncoated sample.

5. Conclusions

The study explores SiO2 and TiO2 nanoparticles synthesized in capped coating using cost-effective sol-gel Strober methods. Using capped dielectric nanoparticles has shown to be a practical, cost-effective approach to enhance the efficiency of silicon solar cells. FESEM images reveal that agglomeration of SiO2 is better than TiO2 nano spherical surface morphology, leading

to efficiency and short circuit current density due to more photon injection caused due to plasmonic confinement with continuous reflection from surrounding agglomerations of capped nanoparticles on the glass surface. These capped dielectric nanoparticle-based silicon solar cells are irradiated under AM1.5 equivalent white light illuminated conditions. Low coating dosages of SiO2-induced photonic absorption increase JSC (short-circuit current density) and PCE (photo-conversion efficiency), improving their overall efficiency compared to titania-induced photonic irradiation.

Compared to the uncoated silicon photovoltaic cell, coating of the first dose of SiO2: 0.693mg/ml concentration improves efficiency at 2.45%, whereas second dose of SiO2: 0.485mg/ml concentration improves efficiency at 1.06%. Similarly, compared with bared silicon solar cells, coating of the first dose of TiO2: 0.525 mg/ml concentration improved efficiency at 0.657%, whereas the second dose of TiO2: 0.748 mg/ml concentration improved efficiency at 0.406%. Several impacts, like the plasmonic effect, low ohmic loss, and improvement in phase matching, reveal a collective gain in efficiency at 8.69% for SiO2 nanoparticles and 6.89% for TiO2 nanoparticles based on various sample dosages. Increased dosage concentration decreases photo-conversion efficiency. The increased light-trapping ability of the cell, combined with the ability to tune the wavelength, makes this approach a promising one for future solar cell study.

References

[1] International Technology Roadmap for Photovoltaic [Internet] 2023. Available from: http://www.itrpv.net/Reports/Downloads/
[2] A. Ali, H. Park, R. Mall, B. Aïssa, S. Sanvito, H. Benzamil, A. Belaidi, F. El-Mellouhi, Chem. Mater. **32**,2998(2020); https://doi.org/10.1021/acs.chemmater.9b05342
[3] M. Liang, A. Ali, A. Belaidi, M.I. Hossain, O. Ronan, C. Downing, N. Tabet, S. Sanvito, F. Ei-Mellouhi, and V. Nicolosi, npj 2D Materials and Applications **4**(40), 1(2020); https://doi.org/10.1038/s41699-020-00173-1
[4] A. Allouhi, S. Rehman, M. Sami Buker, and Z. Said, Journal of Cleaner Production **362**, 132339(2022); https://doi.org/10.1016/j.jclepro.2022.132339
[5] E. T. Efaz, M. Rhaman, S. Al Imam, K. L. Bashar, F. Kabir, E. Mourtaza, S. N. Sakib and F. A. Mozahid, Engineering Research Express **3**(3),032001(2021); https://doi.org/10.1088/2631-8695/ac2353
[6] S. Philips, Fraunhofer Institute for Solar Energy Systems, ISE, Freiburg, Germany, 2019; https://www.ise.fraunhofer.de/content/dam/ise/de/documents/publications/studies/Photovoltaics-Report.pdf.
[7] V.E. Ferry, J.N. Munday, and H. A. Atwater, Advanced Materials **22**(43), 4794(2010); https://doi.org/10.1002/adma.201000488
[8] H. Atwater, A. Polman, Nature Materials **9**, 205 (2010); https://doi.org/10.1038/nmat2629
[9] J. Liu, H. He, D. Xiao, S. Yin, W. Ji, S. Jiang, D. Luo, B. Wang, Y. Liu, Materials, **11**(10) 1833(2018); https://doi.org/10.3390/ma11101833
[10] C.M. Cobley, S.E. Skrabalak, and D.J. Campbell, Plasmonics **4**, 171(2009); https://doi.org/10.1007/s11468-009-9088-0
[11] P. Colson, C. Henrist, R. Cloots, and J Nanomater **2013**, 948510(2013); https://doi.org/10.1155/2013/948510
[12] I. G. Gonzalez-Martinez, A. Bachmatiuk, V. Bezugly, J. Kunstmann, T. Gemming, Z. Liu, G. Cuniberti, M. H. Rümmeli, Nanoscale, **8**, 11340(2016); https://doi.org/10.1039/C6NR01941B .
[13] J. Krajczewski, K. K.¸ Taj, A. Kudelsk, RSC Adv., **7,** 17559(2017); https://doi.org/10.1039/C7RA01034F .
[14] L. Yang, J. Wei, Z. Ma, P. Song, J. Ma, Y. Zhao, Z. Huang, M. Zhang, F. Yang, X. Wang, Nanomaterials (Basel, Switzerland), **9**(12), 1789(2019); https://doi.org/10.3390/nano9121789
[15] X. Chen, B. Jia, J.K. Saha, B. Cai, N. Stokes, Q. Qiao, Y. Wang, Z. Shi, M. Gu, Nano Lett., **12**(5), 2187(2012); https://doi.org/10.1021/nl203463z .
[16] J. Olson, S. Dominguez-Medina, A. Hoggard, L. Y. Wang, W. S. Chang, S. Link, Chem. Soc. Rev.,**44**, 40(2015); https://doi.org/10.1039/C4CS00131A

[17] A. Agrawal, I. Kriegel, and D. J. Milliron, J. Phys. Chem. C, **119**(11), 6227(2015); https://doi.org/10.1021/acs.jpcc.5b01648
[18] M. Kim, J. H. Lee, and J. M. Nam, Adv. Sci. **6**, 1900471(2019) https://doi.org/10.1002/advs.201900471
[19] P. West, S. Ishii, G. Naik, N. Emani, V. Shalaev, A. Boltasseva, Laser & Photon. Rev., **4**, 795(2010); https://doi.org/10.1002/lpor.200900055
[20] J. Jana, M. Ganguly, T. Pal, RSC Adv., **6**, 86174(2016);https://doi.org/10.1039/C6RA14173K
[21] A. Derkachova, K. Kolwas, and I. Demchenko, Plasmonics, **11**, 941(2016); https://doi.org/10.1007/s11468-015-0128-7
[22] M. Tzschoppe, C. Huck, J. Vogt, F. Neubrech, A. Pucci, J. Phys. Chem. C, **122**(27), 15678 (2018); https://doi.org/10.1021/acs.jpcc.8b04209
[23] J. K. Bhattarai, M. H. U. Maruf, K. J. Stine, Processes **8**(1), 115(2020); https://doi.org/10.3390/pr8010115
[24] A. Yu, W. S. Akimov, S. Koh, Y. Sian, S. Ren, Appl. Phys. Lett. **96,** 073111(2010); https://doi.org/10.1063/1.3315942 .
[25] A. Yu, W. S. Akimov, S. Koh, K. Ostrikov, Opt. Express **17**, 10195(2009); https://doi.org/10.1364/OE.17.010195 .
[26] C. M. Hsu, C. Battaglia, C. Pahud, Z. Ruan, F. J. Haug, S. Fan, C. Ballif, Y. Cui, Adv. Energy Mater., **2**, 628(2012); https://doi.org/10.1002/aenm.201100514
[27] Y. Yan, J. Fu, L. Xu, T. Wang, X. Lu, Micro & Nano Letters, **11(**12), 885(2016); https://doi.org/10.1049/mnl.2016.0434
[28] P. Sarkar, S. Panda, B. Maji, A. K. Mukhopadhyay, Journal of Ovonic Research, **18**(6), 723(2022); https://doi.org/10.15251/JOR.2022.186.723
[29] Q. D. Truong, L. X. Dien, Dai-Viet N. Vo, T. S. Le, Journal of Solid-State Chemistry, **251**, 143(2017); https://doi.org/10.1016/j.jssc.2017.04.017
[30] K. Tadanaga, K. Morita, and K. Mori, J Sol-Gel Sci Technol, **68**, 341(2013); https://doi.org/10.1007/s10971-013-3175-6
[31] E. D. Palik, "Handbook of Optical Constants of solids," Academic Press, 1985; https://doi.org/10.1016/C2009-0-20920-2
[32] C. D. Geddes, Reviews in Plasmonics 2010, Springer, New York, 2013; https://doi.org/10.1007/978-1-4614-0884-0
[33] L. Si, T. Qiu, W. Zhang and P. K.Chu, Recent Patents on Materials Science , **5**(2), 166(2012); http://dx.doi.org/10.2174/1874464811205020166
[34] S. Kawata, "Near-Field Optics and Surface Plasmon Polariton", Springer. 2001.
[35] P. Sarkar, S. Panda, B. Maji, A. Kr Mukhopadhyay, Proceedings at IEEEXplore digital library of ICCECE 2016, pp1-6; https://doi.org/10.1109/ICCECE.2016.8009538
[36] P. Sarkar, S. Panda, B. Maji, A. Kr Mukhopadhyay, Proceedings at IEEEXplore digital library in DevIC 2017, pp. 175-179; https://doi.org/10.1109/DEVIC.2017.8073931
[37] P. Sarkar, S. Panda, B. Maji, and A. Kr. Mukhopadhyay, International Journal of Nanoparticles, **10(**1/2),77(2018); https://doi.org/10.1504/IJNP.2018.092678
[38] P. Sarkar, A. Manna, S. Panda, B. Maji, A. Kr. Mukhopadhyay, Materials Today: Proceedings, **5**(10), 21225(2018); https://doi.org/10.1016/j.matpr.2018.06.522
[39] P. Sarkar, S. N. Surai, S. Panda, B. Maji, A. Kr Mukhopadhyay, Proceedings in Contemporary Advances in Innovative and Applicable Information Technology, AISC, Springer, **812**, 67(2018); https://doi.org/10.1007/978-981-13-1540-4_8
[40] P. Sarkar, B. Maji, A. Manna, S. Panda, A. Kr Mukhopadhyay, International Journal of Nanoscience, **17**(4)1760028-1(2018); https://doi.org/10.1142/S0219581X17600286
[41] P. Sarkar, S. Panda, B. Maji, A. Kr. Mukhopadhyay, Nanoscience & Nanotechnology-Asia, **10**(4), 425(2020); http://dx.doi.org/10.2174/2210681209666190830100710
[42] P. Sarkar, S. Panda, B. Maji, A. Kr Mukhopadhyay, Proceedings at IEEEXplore digital library in EDKCON18, pp 437-440; https://doi.org/10.1109/EDKCON.2018.8770473